

Integrated Analysis of Circulating miR-22-3p, miR-126-3p, and miR-760 as Non-invasive Biomarkers for Rheumatoid Arthritis

Alireza Raghobi¹, Amirhossein Mohajeri Khorasani^{2,3,4}, Elia Damavandi⁵, Abdolrahman Rostamian⁶,
Mozhgan Abjoushak Mahmoudabad⁷, Hamid Choobineh⁸, Mohsen Ghadami^{1,9,10}, and Majid Kabuli¹

¹ Department of Medical Genetics, School of Medicine, Tehran University of Medical Sciences, Tehran, Iran

² Medical Genetics Research Center, Mashhad University of Medical Sciences, Mashhad, Iran

³ Metabolic Syndrome Research Center, Mashhad University of Medical Sciences, Mashhad, Iran

⁴ Student Research Committee, Mashhad University of Medical Sciences, Mashhad, Iran

⁵ Department of Photodynamic, Medical Laser Research Center, Yara Institute, ACECR, Tehran, Iran

⁶ Rheumatology Research Center, Imam Khomeini Hospital Complex, Tehran University of Medical Sciences, Tehran, Iran

⁷ Department of Biology, Ma. C., Islamic Azad University, Mashhad, Iran

⁸ Department of Medical Laboratory Sciences, School of Allied Medicine, Tehran University of Medical Sciences, Tehran, Iran

⁹ Endocrinology and Metabolism Research Institute, Tehran University of Medical Sciences, Tehran, Iran

¹⁰ Cardiac Primary Prevention Research Center, Tehran Heart Center, Tehran University of Medical Sciences, Tehran, Iran

Received: 8 October 2025; Received in revised form: 9 April 2026; Accepted: 5 May 2026

ABSTRACT

Rheumatoid arthritis (RA) is an autoimmune disease marked by chronic inflammation and progressive joint damage. Early diagnosis is crucial, but current methods lack sensitivity. Circulating microRNAs (miRs), stable in body fluids, have emerged as promising biomarkers. This study aims to evaluate the plasma expression levels of miR-22-3p, miR-126-3p, and miR-760 in patients with RA compared to healthy controls, and to assess their potential as diagnostic biomarkers.

Plasma samples from 50 RA patients and 50 healthy individuals were analyzed using quantitative real-time PCR (qRT-PCR). Correlation of miR expression with disease activity was evaluated, and their diagnostic value was assessed using receiver operating characteristic (ROC) curve analysis. Bioinformatics analysis was conducted to explore the various aspects and functions of the identified miRs.

The plasma levels of miR-22-3p and miR-126-3p were significantly elevated in RA patients compared to healthy controls. Although miR-760 exhibited an upward trend, the increase did not reach statistical significance. miR-126-3p was positively associated with disease activity. ROC analysis showed area under the curve (AUC) of 0.69 for miR-22-3p, 0.72 for miR-126-3p, and 0.61

Corresponding Authors: Mohsen Ghadami, MD, PhD;
Department of Medical Genetics, School of Medicine, Tehran
University of Medical Sciences, Tehran, Iran. Tel: (+98 21) 6405
3568, Fax: (+98 21) 8895 3005 Email: mghadami@tums.ac.ir

Majid Kabuli, MD, PhD;
Department of Medical Genetics, School of Medicine, Tehran
University of Medical Sciences, Tehran, Iran. Tel: (+98 21) 6405
3320, Fax: (+98 21) 8895 3005 Email: mkabuli@yahoo.co.uk/
mkabuli@tums.ac.ir

for miR-760, with the combined panel improving diagnostic accuracy to an AUC of 0.74. Furthermore, functional enrichment analysis suggested that these miRs are predominantly involved in key biological processes, including regulation of gene expression, cell migration, and epigenetic modifications.

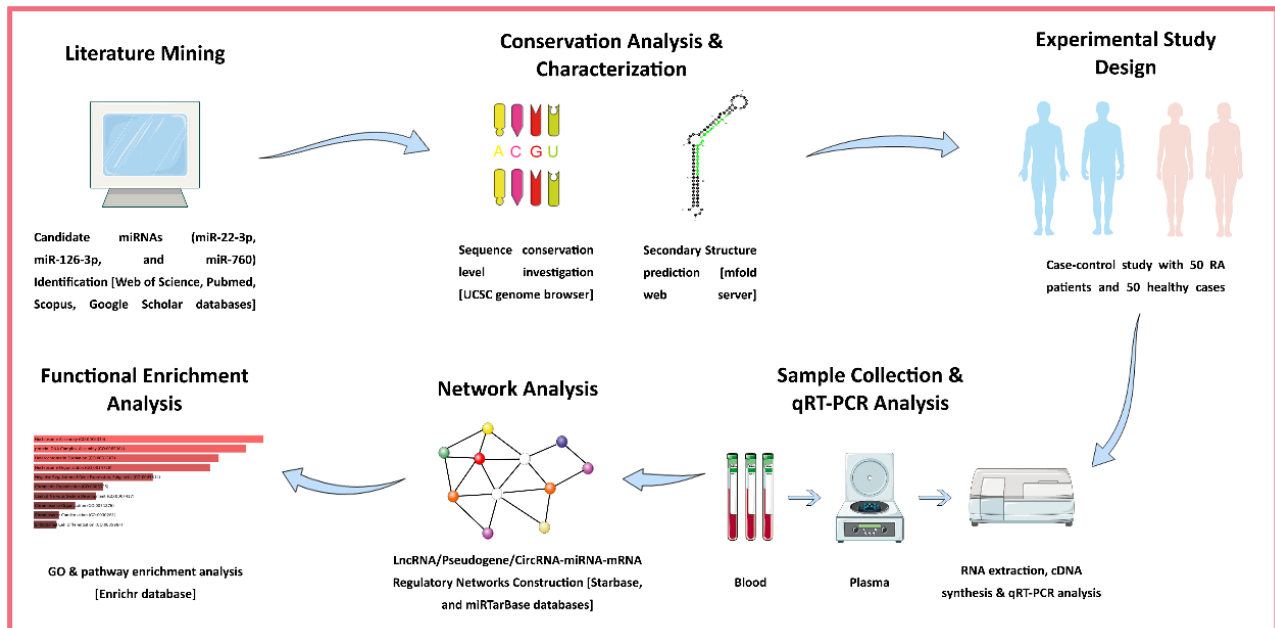
A panel consisting of miR-22-3p, miR-126-3p, and miR-760 may serve as a potential diagnostic biomarker for RA. Further validation in larger and more diverse populations is warranted.

Keywords: Biomarker; MicroRNA; miR-126-3p; miR-22-3p; miR-760; Rheumatoid arthritis

INTRODUCTION

Rheumatoid arthritis (RA) is a chronic autoimmune disorder characterized by symmetrical joint inflammation, which typically begins in the smaller joints and gradually involves larger ones. As the disease advances, it can also impact various organs, including the skin, eyes, heart, kidneys, and lungs. If left untreated, joint damage progressively results in bone erosion and deformities, ultimately leading to severe pain and substantial disability for the patient.¹ RA affects between 0.5% and 1% of adults worldwide, with women being two to three times more likely to develop the condition than men.² It is among the most prevalent autoimmune disorders, yet its main origin remains unclear. It is a highly complex disease influenced by a combination of genetic, epigenetic, and environmental factors.³ The diagnosis of RA is currently based on the American College of Rheumatology/European League

Against Rheumatism (ACR/EULAR) classification criteria. These include an assessment of the number and severity of affected joints, along with laboratory tests such as anti-cyclic citrullinated peptide (anti-CCP), rheumatoid factor (RF), C-reactive protein (CRP), and erythrocyte sedimentation rate (ESR).⁴ However, current diagnostic criteria for RA lack sufficient sensitivity and specificity for early detection, especially in seronegative patients (with negative anti-CCP and RF tests). Some patients in the initial stages of RA do not fulfill the established diagnostic criteria. This can delay diagnosis and treatment, increasing the risk of irreversible joint damage. Moreover, existing tests are not specific to RA and may yield positive results in other autoimmune diseases.⁵ Therefore, it is essential to identify and develop novel diagnostic and prognostic biomarkers to improve the early detection and management of RA.



Graphical Abstract

MicroRNAs (miRs) are small, non-coding RNA molecules that regulate gene expression by binding to the 3' untranslated region (3'UTR) of target mRNAs, leading to their degradation or inhibition of translation. They are critical regulators of various biological processes, including development, cellular differentiation, and signal transduction pathways.⁶ Circulating miRs (c-miRs) are a distinct group of miRs released into body fluids like blood, plasma, urine, and saliva. They exist within extracellular vesicles, or are bound to carrier proteins such as AGO2 or high-density lipoprotein (HDL), which protect them from enzymatic degradation and ensure their stability in the extracellular environment.⁷ Specific c-miR expression patterns can indicate the presence of early-stage diseases, track the progression of more advanced stages, predict disease outcomes, and provide insights into resistance to therapies. As a result, this group of miRs has been extensively investigated as non-invasive diagnostic biomarkers across a wide range of diseases.⁸ RA is no exception to this line of research, as numerous c-miRs have been studied for their potential as biomarkers, particularly in plasma and serum samples. These c-miRs have been proposed as promising candidates for both diagnosing RA and evaluating the disease activity.⁹

Following a comprehensive review of the literature, this study selected miR-22-3p, miR-126-3p, and miR-760 as candidate c-miRs for further evaluation in patients with RA. Although these miRs have been proposed as potential diagnostic biomarkers, their reproducibility and clinical relevance have not been sufficiently validated across diverse populations. Furthermore, the inconsistency between their expression profiles in plasma and those reported in RA-related tissues highlights a critical knowledge gap. To address these uncertainties, the present study systematically evaluated the expression profiles and potential clinical relevance of these selected miRs. In this study, we assessed plasma levels of the mentioned miRs in RA patients and healthy controls, exploring their associations with disease activity and, for the first time, their combined potential as a diagnostic biomarker panel. Moreover, our bioinformatics analysis examined multiple aspects of these miRs, including their conservation, regulatory networks, and potential roles in biological processes and pathways.

MATERIALS AND METHODS

Candidate miRs Identification

To compile a comprehensive list of miRs, a literature mining approach was employed. This literature review-based methodology involved the retrieval of miRs with potential as noninvasive biomarkers for rheumatoid arthritis. Relevant studies were identified through systematic searches of the Web of Science, PubMed, and Scopus databases, as well as the Google Scholar search engine from 2010 to 2025, using the following keywords: "rheumatoid arthritis", "miRNA", "plasma", and "serum".

miR-22, miR-126, and miR-760 Conservation Analysis

The conservation of the *hsa-miR-22*, *hsa-miR-126*, and *hsa-miR-760* genes among vertebrates was evaluated using the UCSC Genome Browser (GRCh38/hg38 human genome assembly).^{10,11}

miR-22, miR-126, and miR-760 Characterization

To characterize the fundamental features of the selected miRs (miR-22-3p, miR-126-3p, and miR-760), we employed the NCBI Gene and Nucleotide databases, as well as the miRBase database.¹² For secondary structure prediction and localization of mature miR sequences within their precursors (pre-miRs), the RNA folding form section of the mfold web server was utilized.¹³ In these visualizations, mature miR regions were highlighted in green, facilitating precise interpretation of their structural configuration. This analysis provided a comprehensive understanding of the spatial organization and secondary structures of the miRs.

Study Population

This case-control study included 50 RA patients and 50 matched healthy controls. Before sample collection, all participants completed a questionnaire capturing key parameters such as height, weight, smoking status, and dietary habits. This information was subsequently utilized to identify and select appropriate healthy controls. RA was diagnosed using ACR/EULAR criteria, with exclusions for major comorbidities and recent infection. Clinical and laboratory parameters (ESR, CRP, RF, anti-CCP, tender joint count [TJC], and swollen joint count [SJC]) were recorded. The study was

approved by the Ethics Committee of Tehran University of Medical Sciences (approval code: IR.TUMS.IKHC.REC.1402.239), and written informed consent was obtained from all participants.

Sample Collection and RNA Extraction

Peripheral venous blood (3 mL) was collected from patients and controls in EDTA tubes. Plasma was isolated through two-step centrifugation (4000g and 14 000g, 10 minutes each, 4°C) to remove cellular debris. The isolated plasma was transferred to RNase/DNase-free microtubes, aliquoted, and stored at -70°C. From each sample, 300 µL of plasma was used for total RNA extraction with YZol reagent (Yekta Tajhiz Azma, Iran), and RNA concentration and purity were assessed using a NanoDrop 2000 spectrophotometer (Thermo Fisher Scientific, USA).

cDNA Synthesis and Quantitative Real-Time PCR (qRT-PCR)

cDNA synthesis was performed using a commercial reverse transcription kit (Karmania Pars Gene, Iran) containing a single-tube master mix without primers. A total of 3.5 µL of extracted RNA was mixed with 7 µL of cDNA master mix and 0.5 µL of stem-loop RT primer. The reaction was run in a thermocycler (Applied Biosystems, USA) at 25°C for 10 minutes, 45°C for 60 minutes, and 95°C for 5 minutes. 1 µL of synthesized cDNA was used for real-time PCR, with the remainder stored at -70°C. qRT-PCR was performed using SYBR Green qPCR Master Mix 2X (Yekta Tajhiz Azma, Iran) on a LightCycler 96 system (Roche, Germany). Each 12 µL reaction contained 1 µL cDNA, 0.5 µL forward primer, 0.5 µL reverse primer, 4 µL distilled water, and 6 µL SYBR Green Master Mix. Primer sequences are listed in Supplementary Table 1.

Cycling conditions were 95°C for 900 seconds, followed by 42 cycles of 95°C for 20 seconds, 58°C for 20 seconds (60°C for miR-760), and 72°C for 45 seconds. Primer amplification efficiency was determined via a standard curve generated from a 10-fold serial dilution (1 to 10⁻⁴) of pooled cDNA for each target. The efficiency (E) was calculated using the formula $E=10^{-1/\text{slope}}$. For additional confirmation, raw fluorescence data from all samples were analyzed with LinRegPCR software. Specificity and product integrity were verified by melting curve analysis and 2.5% agarose gel electrophoresis. Relative expression was calculated using the 2^{-ΔΔC_t} method with U6 as a control.

LncRNA/Pseudogene/CircRNA-miR-mRNA Regulatory Networks

To investigate the regulatory roles of miR-22, miR-126, and miR-760, a Competing Endogenous RNA (ceRNA) network was systematically constructed. Experimentally validated target mRNAs were identified using the multiMIR package, incorporating data from the miRTarBase database.¹⁴ Data analysis was carried out using the R programming software (version R-4.2.1, 64-bit)¹⁵ in combination with RStudio Desktop (version 2022.07.0 Build 548).¹⁶ We obtained the corresponding miR-targeting LncRNAs/Pseudogenes/CircRNAs from the StarBase v.2.0 database.¹⁷ Ultimately, the Cytoscape software (version 3.9.1)¹⁸ was employed to construct the LncRNA/Pseudogene/CircRNA-miR-mRNA ceRNA axis, with the aid of the CytoHubba app¹⁹ to identify central nodes within the network.

Functional Enrichment Analysis

To investigate the potential biological functions of the final set of protein-coding genes directly targeted by miRs, we performed enrichment analyses on the corresponding mRNAs (the full list of mRNA identifiers is provided in Supplementary Material 1). Gene Ontology (GO) enrichment analysis was conducted across 3 categories: cellular component (CC), molecular function (MF), and biological process (BP). Additionally, pathway enrichment analyses were conducted using curated databases including the Kyoto Encyclopedia of Genes and Genomes (KEGG), WikiPathways, and Reactome. All enrichment analyses were performed using the Enrichr tool²⁰ and visualized with ggplot2 in R.²¹ Only terms with adjusted $p < 0.05$ were discussed in the results.

Statistical Analysis

Descriptive statistics (mean ± SD) were used to summarize data. Normality was tested using Kolmogorov-Smirnov and Shapiro-Wilk tests. Depending on the distribution, parametric (*t* test, ANOVA) or nonparametric (Mann-Whitney, Kruskal-Wallis) tests were applied. Correlations were assessed using Pearson or Spearman methods. Receiver operating characteristic (ROC) curve analysis was conducted to evaluate the diagnostic performance of individual miRs and to determine optimal cutoff values. A combined multi-miR diagnostic panel was constructed using multivariable logistic regression analysis, with disease status (rheumatoid arthritis vs control) as the dependent

variable and the expression levels of miR-22-3p, miR-126-3p, and miR-760 ($-\Delta\text{Ct}$ values) as independent variables. Regression coefficients and the intercept were obtained from the logistic regression model. For each subject, a composite diagnostic score was calculated according to the logistic regression equation:

$$\text{Logit}(P) = \beta_0 + \beta_1(\text{miR-22-3p}) + \beta_2(\text{miR-126-3p}) + \beta_3(\text{miR-760})$$

The predicted probability $[P = \exp(\text{Logit}(P)) / (1 + \exp(\text{Logit}(P)))]$ was subsequently used as the test variable for ROC curve analysis of the combined miR panel.

RESULTS

Candidate miRs Identification

A list of 22 candidate miRs suitable for our study was identified through comprehensive literature mining using multiple online databases and search platforms (Supplementary Material 2). Among these, the circulating forms of miR-22-3p, miR-126-3p, and miR-760 were selected for further analysis due to the need for additional validation of their reported reproducibility across diverse populations, especially in Iranian people. Furthermore, discrepancies between their expression profiles in plasma samples and those observed in RA-associated tissues highlight the need for further investigation to elucidate their biomarker potential.

miR-22, miR-126, and miR-760 Conservation Analysis

Comparative genomic analysis revealed that miR-22 and miR-126 exhibit a high degree of evolutionary conservation across vertebrate species, whereas miR-760 displays comparatively lower conservation levels. Notably, all three miRs are highly conserved in specific vertebrates, including humans, rhesus macaques, dogs, elephants, and mice, suggesting their potential significance in fundamental physiological processes across these species (Figure 1).

miR-22, miR-126, and miR-760 Characterization

Using the mfold Web Server, the optimal secondary structures of the pre-miRs for miR-22, miR-126, and miR-760 were predicted based on calculations of their minimum free energy (MFE) values. Furthermore, the specific regions within each precursor from which the corresponding mature miRs are derived are indicated within the predicted secondary structures (Figure 2).

Table 1 summarizes the characteristics of the analyzed miRs.

Demographic and Clinical Characteristics of the Participants

Table 2 summarizes the demographic and clinical characteristics of 50 RA patients and 50 age- and sex-matched healthy controls. Both groups had a mean age of approximately 50 years (RA: 50.04 ± 10.7 ; controls: 50.14 ± 10.6) and identical sex distribution (15 males, 35 females). The mean disease duration among RA patients was 8.9 ± 7.4 years. Inflammatory markers were elevated (CRP: 31.4 ± 29 mg/dL; ESR: 31.1 ± 15.9 mm/h). Anti-CCP and RF positivity were observed in 66% and 74% of patients, respectively. The mean DAS28 was 4.2 ± 1.5 , with varying disease activity levels.

miR-22-3p, miR-126-3p, and miR-760 Differential Expression

Plasma expression levels of miR-22-3p and miR-126-3p were significantly elevated in patients with RA compared to healthy controls, with fold changes of 2.3 and 2.4, respectively ($p=0.0006$ and $p<0.0001$, respectively). Although miR-760 exhibited an upward trend in RA patients, the difference did not reach statistical significance ($p=0.1$) (Figure 3A).

miR-22-3p, miR-126-3p, and miR-760 Expression Differences According to RF, Anti-CCP, and DAS28

No significant differences in miR expression were found between RF-positive and RF-negative patients. However, miR-22-3p and miR-126-3p were significantly upregulated in RF-positive patients compared to healthy controls ($p=0.0005$ and $p<0.0001$, respectively) (Figure 3B).

No significant differences were observed between anti-CCP-positive and anti-CCP-negative patients. However, miR-22-3p and miR-126-3p were significantly elevated in anti-CCP-positive ($p=0.009$ and $p=0.005$, respectively) and anti-CCP-negative patients ($p=0.001$ and $p<0.0001$, respectively) compared to healthy controls. In contrast, miR-760 showed no significant differences across any RF or anti-CCP subgroups (Figure 3C).

miR-22-3p, miR-126-3p, and miR-760 as RA Biomarkers

Table 1. Basic details of the miR-22, miR-126, and miR-760.

Pre-miRs	miRBase accession number	Genomic position, nt	Minimum free energy, kCal/moL	Mature miRs	Mature miR sequence, nt
<i>hsa-miR-22</i>	MI0000078	chr17: 1713903-1713987 [-] (85)	-39.8	<i>hsa-miR-22-3p</i>	AAGCUGCCAGUUGAAGAACUGU (22)
				<i>hsa-miR-22-5p</i>	AGUUCUUCAGUGGCAAGCUUUA (22)
<i>hsa-miR-126</i>	MI0000471	chr9: 136670602-136670686 [+] (85)	-39.6	<i>hsa-miR-126-3p</i>	UCGUACCGUGAGUAAUAAUGCG (22)
				<i>hsa-miR-126-5p</i>	CAUUAUUACUUUUGGUACGCG (21)
<i>hsa-miR-760</i>	MI0005567	chr1: 93846832-93846911 [+] (80)	-41.6	<i>hsa-miR-760</i>	CGGCUCUGGGUCUGUGGGGA (20)

miR: microRNA; nt: nucleotide

Table 2. Participants' demographics and clinical data.

Variables	Controls (n=50)	Patients (n=50)
Sex, male/female	15/35	15/35
Age, mean ± SD, y	50.14 ± 10.6	50.04 ± 10.7
Disease duration, mean ± SD, y	NA	8.9 ± 7.4
CRP, mean ± SD, mg/dL	NA	31.4 ± 29
ESR, mean ± SD, mm/h	NA	31.1 ± 15.9
Anti-CCP positive, No. (%)	NA	33 (66)
RF positive, No. (%)	NA	37 (74)
TJC, mean ± SD	NA	9.4 ± 9.6
SJC, mean ± SD	NA	6.2 ± 7.1
DAS28, mean ± SD	NA	4.2 ± 1.5
Remission, No. (%)	NA	7 (14)
Low activity, No. (%)	NA	11 (22)
Moderate activity, No. (%)	NA	13 (26)
High activity, No. (%)	NA	19 (38)

anti-CCP: anti-cyclic citrullinated peptide; CRP: C-reactive protein; DAS28: Disease Activity Score 28; ESR: erythrocyte sedimentation rate; NA: not available; RF: rheumatoid factor; SD: standard deviation; SJC: swollen joint count; TJC: tender joint count.

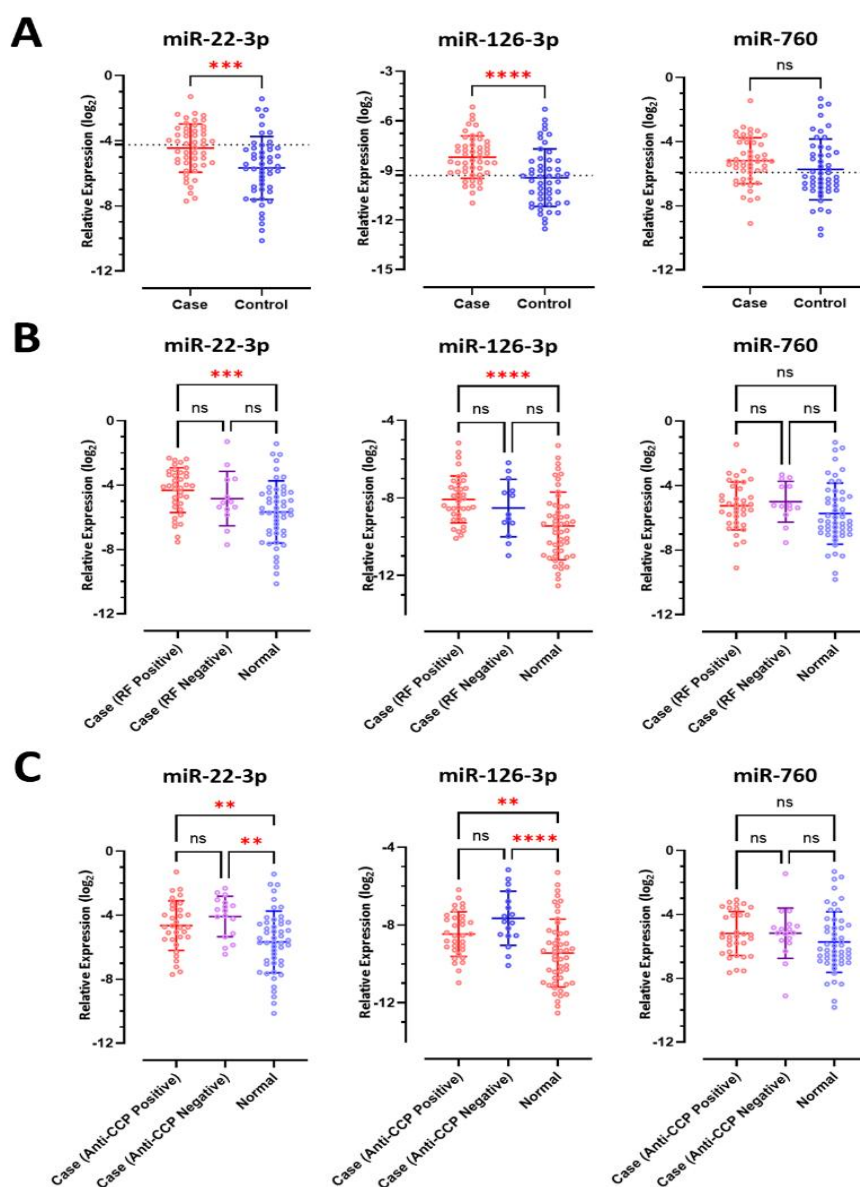


Figure 3. Differential expression of miR-22-3p, miR-126-3p, and miR-760 in plasma samples. A. Relative expression levels of the indicated miRs in patients with RA compared to healthy controls. B. Comparative expression profiles of the miRs in RA patients stratified by RF status versus healthy controls. C. Comparative expression profiles of the miRs in RA patients stratified by anti-CCP antibody status versus healthy controls. ns: not significant.

According to DAS28-based classification (Table 3), miR-22-3p expression was significantly higher in patients with high disease activity compared to healthy controls ($p=0.0005$). miR-126-3p levels were elevated in both high ($p<0.0001$) and moderate ($p=0.008$) activity groups versus controls, and were significantly higher in patients with high activity compared to those with low activity ($p=0.02$) and remission ($p=0.02$) (Figure 4).

miR-22-3p, miR-126-3p, and miR-760 Expression Correlation with DAS28 and Other Clinical Characteristics

Correlation analysis indicated that miR-22-3p was positively and significantly associated exclusively with CRP levels. miR-126-3p exhibited significant positive correlations with DAS28, ESR, and CRP. Conversely, miR-760 demonstrated a significant positive correlation

miR-22-3p, miR-126-3p, and miR-760 as RA Biomarkers

solely with ESR. The corresponding correlation coefficients (r-values) and *p* are provided in Figure 5.

miR-22-3p, miR-126-3p, and miR-760 Diagnostic Potential in RA Patients

ROC curve analysis was performed to assess the diagnostic potential of the studied miRs. The area under

the curve (AUC) values for each miR were calculated, with optimal cutoffs determined using the Youden index. Diagnostic metrics for individual miRs are presented in Table 4. The combined analysis of all three miRs as a biomarker panel showed the highest diagnostic accuracy, achieving an AUC of 0.74 (*p*<0.0001) (Figure 6).

Table 3. Relative expression of miRs according to DAS28 score.

Disease activity (DAS28)	miR-22-3p, mean ± SD	miR-126-3p, mean ± SD	miR-760, mean ± SD
Remission (<2.6)	4.5±2.0	9.0±1.2	5.6±1.5
Low activity (2.6–3.2)	4.8±1.4	8.8±1.3	5.3±1.4
Moderate activity (3.2–5.1)	4.8±1.3	8.1±1.1	5.2±0.8
High activity (>5.1)	3.9±1.3	7.5±1.1	4.9±1.7

DAS28: Disease Activity Score 28; miR: microRNA; SD: standard deviation.

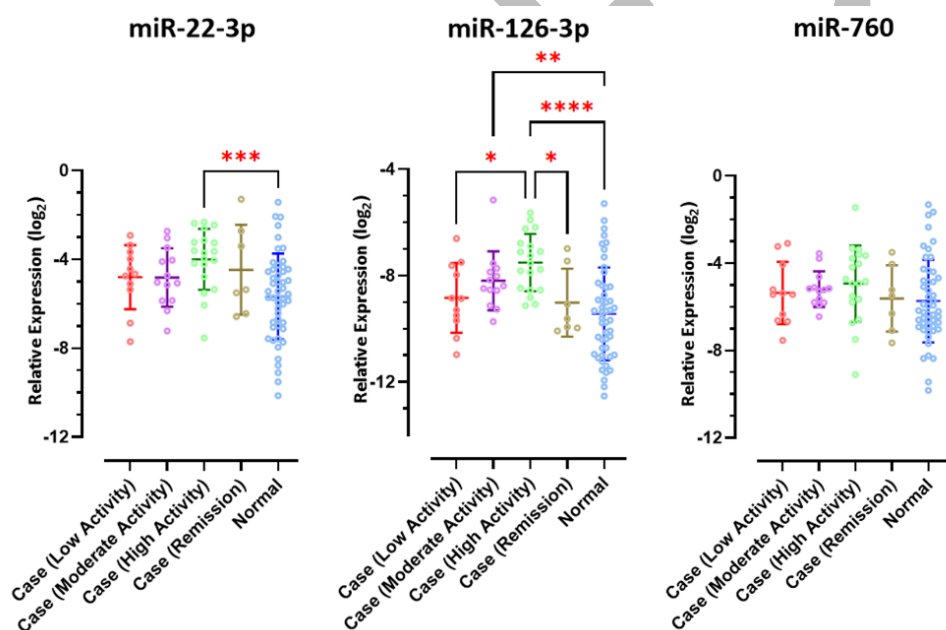


Figure 4. miR-22-3p, miR-126-3p, and miR-760 expression differences according to DAS28.

Table 4. Diagnostic value of miRs.

miR	AUC	Sensitivity	Specificity	<i>p</i>
miR-22-3p	0.69	0.52	0.82	0.0008
miR-126-3p	0.72	0.82	0.58	0.0001
miR-760	0.61	0.76	0.56	0.04

AUC: area under the curve; miR: microRNA.

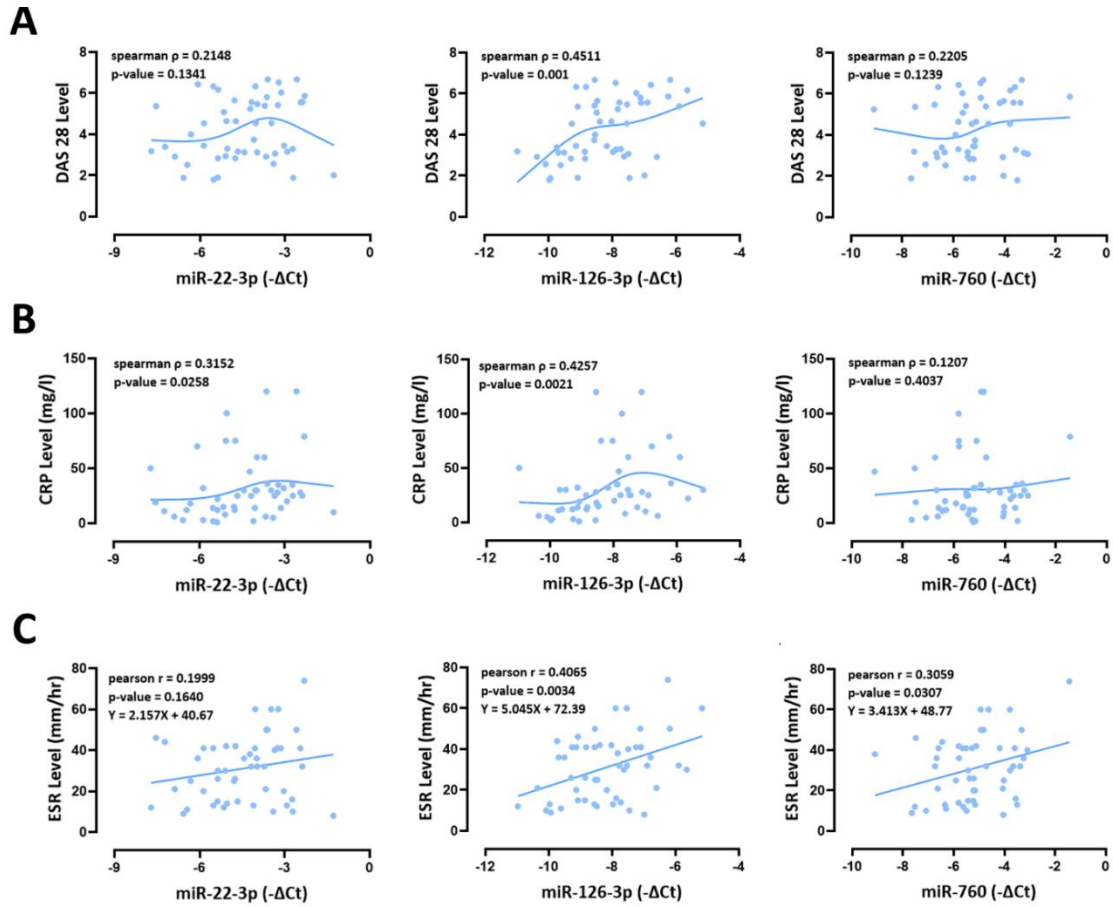


Figure 5. miR-22-3p, miR-126-3p, and miR-760 expression correlation with A. DAS28, B. CRP, and C. ESR.

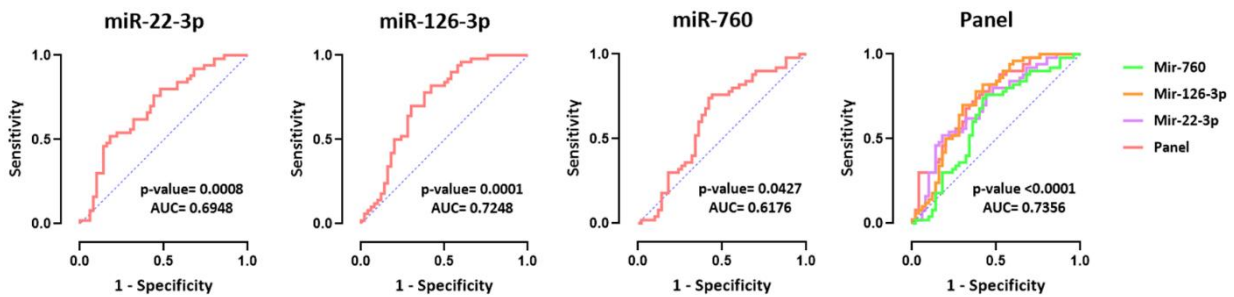


Figure 6. miR-22-3p, miR-126-3p, and miR-760 diagnostic potential in RA patients.

Absolute Risk Calculation Based on miR-22-3p, miR-126-3p, and miR-760 Differential Expression

Absolute risk was calculated for each miR using the formula proposed by Zamani et al, which estimates predicted positive (PPV) and negative (NPV) values based on disease prevalence.²² Based on a study by Davatchi et al, an RA prevalence of 0.37% in Iran was applied,²³ and a cut-off derived from the mean expression of miR levels was used to classify samples

as positive or negative. The resulting PPV and NPV values for each miR are presented in Table 5. Given the low prevalence of the disease in the studied population, low PPV values are expected. In contrast, the high NPV values indicate that changes in the expression of these miRs, in combination with other diagnostic approaches, may be useful for ruling out the disease in healthy individuals.

Table 5. Positive and negative predicted values based on miR expression.

miR	Negative predicted values (NPV)	Positive predicted values (PPV)
miR-22-3p	0.997	0.006
miR-126-3p	0.998	0.007
miR-760	0.997	0.006

miR: microRNA; NPV: negative predicted value; PPV: positive predicted value.

LncRNA/Pseudogene/CircRNA-miR-mRNA Regulatory Networks

Based on the maximal clique centrality (MCC) algorithm, the top 10 regulatory molecules were identified within the miR-centered interaction network. Among these, hsa-miR-22-3p, hsa-miR-126-3p, and hsa-miR-760 achieved the highest MCC scores, suggesting their prominent centrality and potential regulatory significance within the networks. These results are illustrated in Figure 7 and summarized in Table 6.

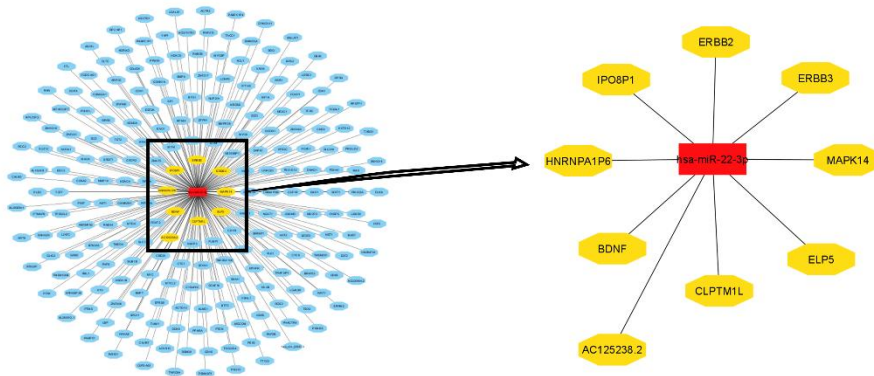
Functional Enrichment Analysis

To gain a deeper understanding of the molecular mechanisms underlying the protein-coding genes directly targeted by miRs, we performed comprehensive Gene Ontology (GO) enrichment analyses for each miR-targeted gene set. For the miR-22-3p-targeted gene set, significant enrichment was observed in biological processes such as regulation of gene expression and negative regulation of DNA-templated transcription. Furthermore, this gene set was highly associated with molecular functions, including kinase binding and RNA polymerase II-specific DNA-binding transcription factor binding. In terms of cellular component

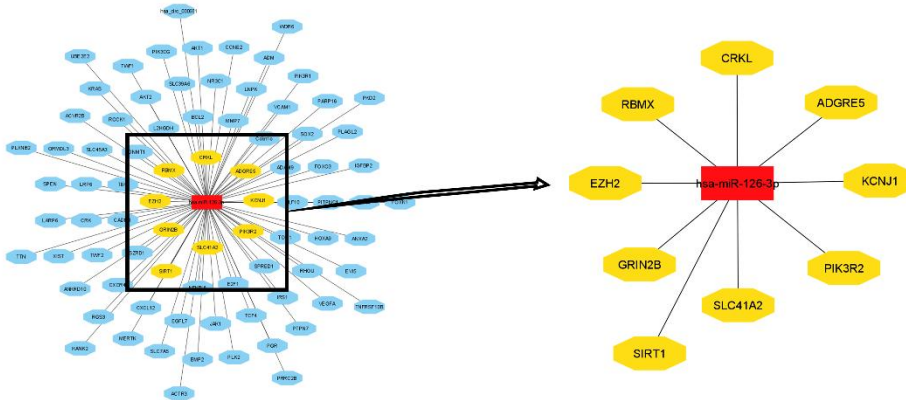
distribution, the majority of these genes were localized to the nucleus and intracellular membrane-bounded organelles. Pathway enrichment analysis using KEGG, WikiPathways, and Reactome databases revealed the top 10 enriched pathways, which included signal transduction, cellular responses to stimuli, gene expression (transcription), pathways in cancer, and cellular senescence (Figure 8).

The miR-126-3p-targeted gene set showed significant enrichment in biological processes such as positive regulation of cell migration and positive regulation of small molecule metabolic process. Enriched molecular functions included phosphotyrosine residue binding, receptor tyrosine kinase binding, and protein phosphorylated amino acid binding. These genes were predominantly localized in the phosphatidylinositol 3-kinase complex, class I, as well as the nucleus and intracellular membrane-bounded organelles. The top 10 enriched pathways for this gene set comprised signaling by interleukins, chemokine signaling pathway, pathways in cancer, and signal transduction (Figure 9).

A



B



C

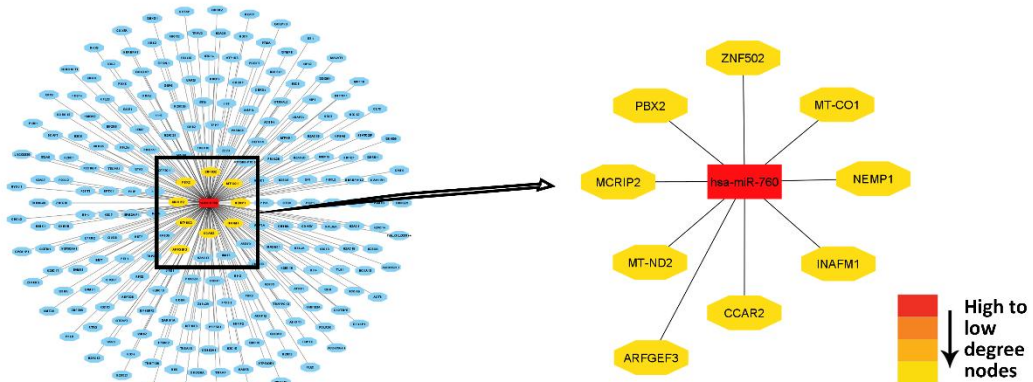


Figure 7. LncRNA/Pseudogene/CircRNA-miR-mRNA regulatory networks for A. hsa-miR-22-3p, B. hsa-miR-126-3p, and C. hsa-miR-760. The MCC score, ranging from high to low, was shown by the red to yellow spectrum.

miR-22-3p, miR-126-3p, and miR-760 as RA Biomarkers

Table 6. Top 10 nodes within the LncRNA/pseudogene/CircRNA-miR-mRNA interaction network, ranked according to the MCC algorithm.

Network	Rank	Node name	Score
hsa-miR-22-3p	1	hsa-miR-22-3p	227
	2	AC125238.2	1
	2	<i>ERBB3</i>	1
	2	IPO8P1	1
	2	<i>ERBB2</i>	1
	2	HNRNPA1P6	1
	2	<i>MAPK14</i>	1
	2	<i>ELP5</i>	1
	2	<i>BDNF</i>	1
	2	<i>CLPTMIL</i>	1
hsa-miR-126-3p	1	hsa-miR-126-3p	82
	2	<i>ADGRE5</i>	1
	2	<i>CRKL</i>	1
	2	<i>GRIN2B</i>	1
	2	<i>PIK3R2</i>	1
	2	<i>SLC41A2</i>	1
	2	<i>EZH2</i>	1
	2	<i>RBMX</i>	1
	2	<i>SIRT1</i>	1
2	<i>KCNJ1</i>	1	
hsa-miR-760	1	hsa-miR-760	227
	2	<i>INAFM1</i>	1
	2	<i>MCRIP2</i>	1
	2	<i>ARFGEF3</i>	1
	2	<i>ZNF502</i>	1
	2	<i>NEMP1</i>	1
	2	<i>CCAR2</i>	1
	2	<i>PBX2</i>	1
	2	<i>MT-CO1</i>	1
	2	<i>MT-ND2</i>	1

CircRNA: circular RNA; LncRNA: long noncoding RNA; MCC: maximal clique centrality; miR: microRNA; mRNA: messenger RNA.

miR-22-3p, miR-126-3p, and miR-760 as RA Biomarkers

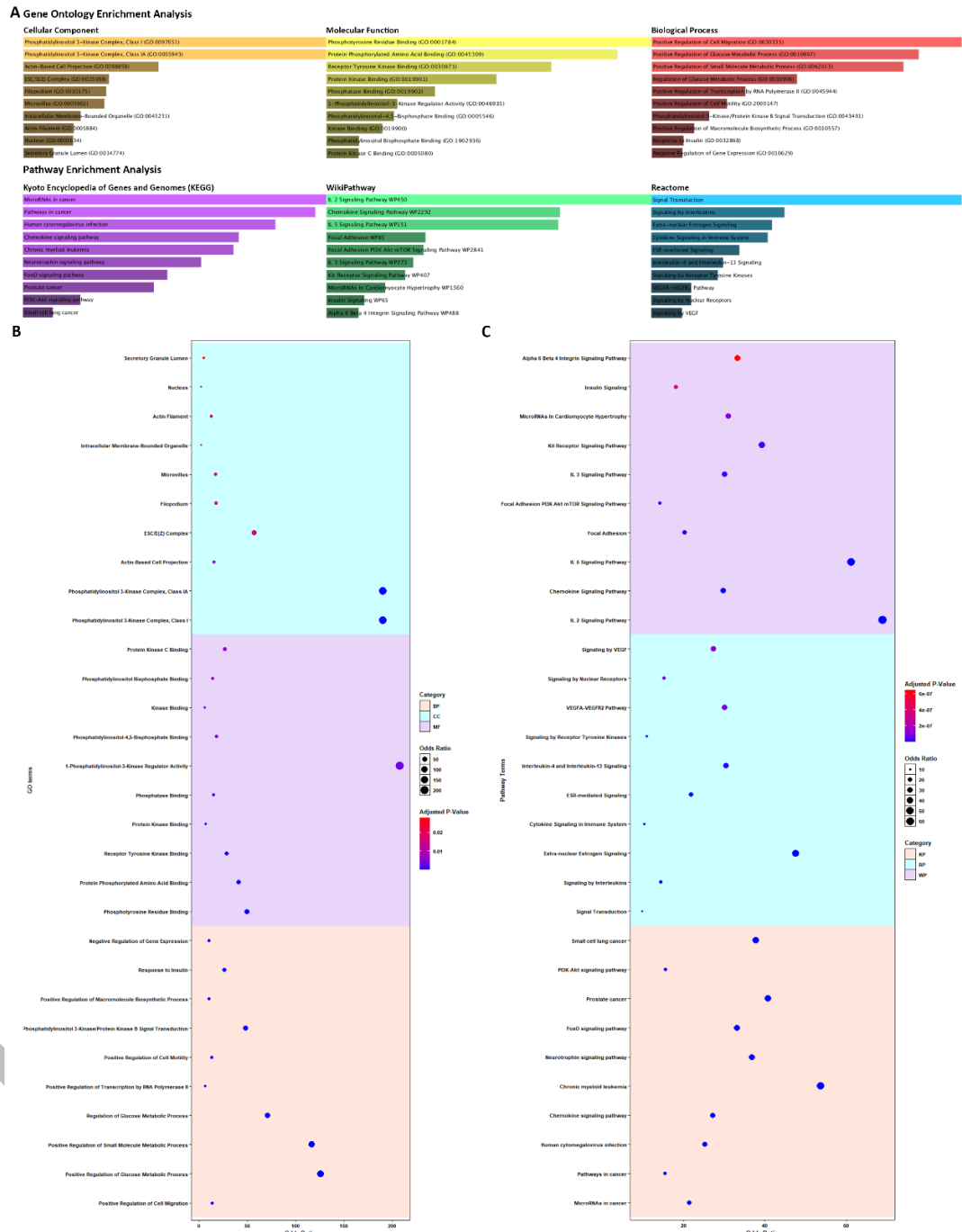


Figure 9. The miR-126-3p-related gene set enrichment analysis. The GO enrichment analysis and pathway enrichment analysis from the Enrichr tool were visualized by bar plot (A) and dot plots (B, C).

For the miR-760-targeted gene set, the most significantly enriched biological processes included protein-DNA complex assembly, negative regulation of gene expression (epigenetic), and nucleosome assembly. In terms of molecular function, nucleosomal DNA binding was the only significant function. The

genes were mainly localized to the nucleus and intracellular membrane-bounded organelles. The top 10 enriched pathways included neutrophil extracellular trap formation, DNA damage/telomere stress-induced senescence, DNA methylation, histone modifications, and cellular senescence (Figure 10).

combined diagnostic value. Moreover, our bioinformatics analysis examined multiple aspects of these miRs.

In our study, miR-22-3p was significantly elevated in the plasma of RA patients, including anti-CCP-negative cases, suggesting diagnostic potential in seronegative RA. It also correlated with CRP levels and showed moderate diagnostic performance with an AUC of 0.69. Tang et al reported that miR-22-3p was significantly upregulated in RA patients and distinguished them from SLE and Sjögren's cases, with an AUC of 0.81, underscoring its diagnostic value, particularly in seronegative RA.³⁰ Another study confirmed elevated plasma miR-22-3p levels in RA patients compared to healthy controls, with a strong association with disease activity.³¹ Similarly, Ormseth et al found increased plasma expression of miR-22-3p, significantly correlating with DAS28 and disease activity.³² Its upregulation was also noted in peripheral blood cells of RA patients.³³

Alternatively, the miR-126-3p was significantly elevated in RA patients and could distinguish anti-CCP-negative cases from controls. It correlated with ESR, CRP, and DAS28, indicating links to inflammation and disease activity. Its diagnostic value was moderate, with an AUC of 0.72. Cunningham et al reported elevated miR-126-3p in RA patients and at-risk individuals compared to controls, indicating its potential as an early diagnostic biomarker with strong accuracy (AUC: 0.87 for RA, 0.76 for at-risk cases).³⁴ Given that cardiovascular disease is a major RA complication, miR-126-3p may also serve as a predictive marker for coronary atherosclerosis in RA patients.³⁵

Plasma miR-760 expression levels were found to be elevated in patients with RA compared to healthy controls; however, this difference did not reach statistical significance. Moreover, plasma miR-760 levels demonstrated a positive correlation with ESR. In a study conducted by Abdelaleem et al, serum miR-760 expression was reported to be significantly increased in RA patients within an Egyptian cohort, with an AUC of 0.85, indicating its potential diagnostic utility.³⁶ Conversely, another study reported a decrease in miR-760 expression in T cells derived from RA patients, suggesting a possible cell-type-specific regulation and highlighting the complex role of miR-760 in RA pathogenesis.³⁷

Among the three analyzed miRs, miR-126-3p exhibited the highest diagnostic accuracy, whereas miR-

760 demonstrated the lowest. Notably, the combined assessment of all three miRs as a diagnostic panel yielded the greatest overall diagnostic performance. This observation is consistent with previous studies, which have highlighted the superior diagnostic potential of miR panels compared to the evaluation of individual biomarkers.³⁸⁻⁴³ The plasma levels of miR-22-3p, miR-126-3p, and miR-760 are elevated in RA patients, while their expression is often reduced in tissues or inside cells. This discrepancy is expected, as extracellular miR levels do not always reflect their intracellular abundance. Cells use different selective mechanisms to package and release miRs into the extracellular environment, meaning the profiles of circulating and intracellular miRs can differ significantly. Additionally, circulating miRs may originate from various cell types, making their plasma levels the result of complex and diverse cellular contributions.⁴⁴ Additionally, this difference in expression suggests that these three miRs likely play a complex role in the pathogenesis of RA.

Conservation analysis showed that all three miRs are well preserved among certain vertebrates, indicating their possible importance in fundamental physiological processes across these species. Functional enrichment analysis highlighted distinct complementary roles for the three studied miRs. Target genes of miR-22-3p were enriched in processes related to transcriptional regulation, kinase binding, and pathways such as cancer and cellular senescence, suggesting its involvement in transcriptional control and signaling cascades relevant to inflammation. Overexpression of miR-22-3p in MH7A cells suppressed inflammatory cell activity by targeting IL6R and could be involved in the regulation of the NF- κ B pathway in RA.⁴⁵ In a study on RASF cells, miR-22-3p was found to be significantly downregulated, leading to altered secretion of inflammatory cytokines (IL-6, IL-1 β , and TNF- α) and enhanced cell proliferation through regulation of SIRT1.⁴⁶ It has also been shown that EZH2-mediated hypermethylation of the miR-22-3p promoter suppresses its expression, thereby promoting proliferation, migration, and invasion of RA-FLSs through upregulation of CYR61.⁴⁷ miR-126-3p showed enrichment in functions associated with cell migration, cytokine and chemokine signaling, and receptor tyrosine kinase pathways, consistent with its potential roles in angiogenesis, immune cell trafficking, and synovial inflammation. Downregulation of miR-126-3p in RA-FLS enhances PIK3R2 expression, leading to activation of the PI3K/AKT pathway and increased levels of PI3K,

AKT, and phosphorylated AKT, thereby contributing to synovial angiogenesis in RA.⁴⁸ miR-126-3p can also regulate the NF- κ B signaling pathway in RA-FLS cells by targeting p-p65 and p-I κ B α .⁴⁹ miR-760 was enriched in pathways linked to DNA methylation, nucleosome assembly, and histone modifications, indicating a potential role in epigenetic regulation and cellular senescence, both of which are increasingly recognized in RA pathogenesis.

Given the significant upregulation of miR-22-3p and miR-126-3p in the plasma of RA patients compared to healthy controls, these miRs show promise as potential diagnostic biomarkers for RA. Moreover, combining miR-22-3p, miR-126-3p, and miR-760 as a biomarker panel enhances their overall diagnostic performance. Notably, miR-126-3p expression positively correlates with DAS28 scores, suggesting its utility in assessing disease activity and severity. The study's limitation was the relatively small sample size, which may affect the generalizability of the findings. Future research should aim to validate these results in larger, independent cohorts. Additionally, the lack of access to synovial tissue samples prevented the evaluation of miR expression at the local site of inflammation. Notably, few studies to date have assessed the plasma expression of miR-22-3p, miR-126-3p, and miR-760 in RA patients. Furthermore, the functional roles of these miRs in the pathogenesis and progression of RA remain to be fully elucidated and warrant further investigation.

STATEMENT OF ETHICS

This study was conducted with the approval of the Ethics Committee of Tehran University of Medical Sciences (approval code: IR.TUMS.IKHC.REC.1402.239). Written informed consent was obtained from all participants.

FUNDING

This research was funded by Tehran University of Medical Sciences.

CONFLICT OF INTEREST

The authors declare no conflicts of interest.

ACKNOWLEDGMENTS

Graphical abstract adapted from Servier Medical Art (<https://smart.servier.com/>), licensed under CC BY 4.0 (<https://creativecommons.org/licenses/by/4.0/>).

DATA AVAILABILITY

Data will be available on reasonable request.

AI ASSISTANCE DISCLOSURE

Not applicable.

REFERENCES

1. Bullock J, Rizvi SAA, Saleh AM, Ahmed SS, Do DP, Ansari RA, et al. Rheumatoid Arthritis: A Brief Overview of the Treatment. *Med Princ Pract.* 2018;27(6):501-7.
2. Venetsanopoulou AI, Alamanos Y, Voulgari PV, Drosos AA. Epidemiology and Risk Factors for Rheumatoid Arthritis Development. *Mediterr J Rheumatol.* 2023;34(4):404-13.
3. Scherer HU, Häupl T, Burmester GR. The etiology of rheumatoid arthritis. *Journal of Autoimmunity.* 2020;110:102400.
4. Jang S, Kwon EJ, Lee JJ. Rheumatoid Arthritis: Pathogenic Roles of Diverse Immune Cells. *Int J Mol Sci.* 2022;23(2).
5. Cheng Q, Chen X, Wu H, Du Y. Three hematologic/immune system-specific expressed genes are considered as the potential biomarkers for the diagnosis of early rheumatoid arthritis through bioinformatics analysis. *J Transl Med.* 2021;19(1):18.
6. O'Brien J, Hayder H, Zayed Y, Peng C. Overview of MicroRNA Biogenesis, Mechanisms of Actions, and Circulation. *Front Endocrinol (Lausanne).* 2018;9:402.
7. Pozniak T, Shcharbin D, Bryszewska M. Circulating microRNAs in Medicine. *Int J Mol Sci.* 2022;23(7).
8. Wu Y, Li Q, Zhang R, Dai X, Chen W, Xing D. Circulating microRNAs: Biomarkers of disease. *Clin Chim Acta.* 2021;516:46-54.
9. Peng X, Wang Q, Li W, Ge G, Peng J, Xu Y, et al. Comprehensive overview of microRNA function in rheumatoid arthritis. *Bone Res.* 2023;11(1):8.
10. Kent WJ, Sugnet CW, Furey TS, Roskin KM, Pringle TH, Zahler AM, et al. The human genome browser at UCSC. *Genome research.* 2002;12(6):996-1006.
11. Nassar LR, Barber GP, Benet-Pagès A, Casper J, Clawson H, Diekhans M, et al. The UCSC Genome Browser

miR-22-3p, miR-126-3p, and miR-760 as RA Biomarkers

- database: 2023 update. *Nucleic Acids Research*. 2023;51(D1):D1188-D95.
12. Kozomara A, Birgaoanu M, Griffiths-Jones S. miRBase: from microRNA sequences to function. *Nucleic Acids Res*. 2019;47(D1):D155-d62.
 13. Zuker M. Mfold web server for nucleic acid folding and hybridization prediction. *Nucleic Acids Research*. 2003;31(13):3406-15.
 14. Ru Y, Kechris KJ, Tabakoff B, Hoffman P, Radcliffe RA, Bowler R, et al. The multiMiR R package and database: integration of microRNA-target interactions along with their disease and drug associations. *Nucleic Acids Res*. 2014;42(17):e133.
 15. R Core Team (2022). R: A language and environment for statistical computing. R Foundation for Statistical Computing, Vienna, Austria. URL <https://www.R-project.org/>.
 16. RStudio Team (2022). RStudio: Integrated Development Environment for R. RStudio, PBC, Boston, MA URL <http://www.rstudio.com/>.
 17. Li J-H, Liu S, Zhou H, Qu L-H, Yang J-H. starBase v2.0: decoding miRNA-ceRNA, miRNA-ncRNA and protein-RNA interaction networks from large-scale CLIP-Seq data. *Nucleic Acids Research*. 2013;42(D1):D92-D7.
 18. Shannon P, Markiel A, Ozier O, Baliga NS, Wang JT, Ramage D, et al. Cytoscape: a software environment for integrated models of biomolecular interaction networks. *Genome Res*. 2003;13(11):2498-504.
 19. Chin C-H, Chen S-H, Wu H-H, Ho C-W, Ko M-T, Lin C-Y. cytoHubba: identifying hub objects and sub-networks from complex interactome. *BMC Systems Biology*. 2014;8(4):S11.
 20. Xie Z, Bailey A, Kuleshov MV, Clarke DJ, Evangelista JE, Jenkins SL, et al. Gene set knowledge discovery with enrichr. *Current protocols*. 2021;1(3):e90.
 21. H. Wickham. ggplot2: Elegant Graphics for Data Analysis. Springer-Verlag New York, 2016.
 22. Zamani M, Cassiman JJ. Reevaluation of the importance of polymorphic HLA class II alleles and amino acids in the susceptibility of individuals of different populations to type I diabetes. *American journal of medical genetics*. 1998;76(2):183-94.
 23. Davatchi F, Sandoughi M, Moghimi N, Jamshidi AR, Tehrani Banihashemi A, Zakeri Z, et al. Epidemiology of rheumatic diseases in Iran from analysis of four COPCORD studies. *International journal of rheumatic diseases*. 2016;19(11):1056-62.
 24. Ding Q, Hu W, Wang R, Yang Q, Zhu M, Li M, et al. Signaling pathways in rheumatoid arthritis: implications for targeted therapy. *Signal Transduct Target Ther*. 2023;8(1):68.
 25. Kim JW, Suh CH. Systemic Manifestations and Complications in Patients with Rheumatoid Arthritis. *J Clin Med*. 2020;9(6).
 26. Steiner G, Verschueren P, Van Hoovels L, Studenic P, Bossuyt X. Classification of rheumatoid arthritis: is it time to revise the criteria? *RMD Open*. 2024;10(2).
 27. Metcalf GAD. MicroRNAs: circulating biomarkers for the early detection of imperceptible cancers via biosensor and machine-learning advances. *Oncogene*. 2024;43(28):2135-42.
 28. Gayosso-Gómez LV, Ortiz-Quintero B. Circulating MicroRNAs in Blood and Other Body Fluids as Biomarkers for Diagnosis, Prognosis, and Therapy Response in Lung Cancer. *Diagnostics (Basel)*. 2021;11(3).
 29. Evangelatos G, Fragoulis GE, Koulouri V, Lambrou GI. MicroRNAs in rheumatoid arthritis: From pathogenesis to clinical impact. *Autoimmun Rev*. 2019;18(11):102391.
 30. Tang J, Lin J, Yu Z, Jiang R, Xia J, Yang B, et al. Identification of circulating miR-22-3p and let-7a-5p as novel diagnostic biomarkers for rheumatoid arthritis. *Clin Exp Rheumatol*. 2022;40(1):69-77.
 31. Cieśla M, Kolarz B, Majdan M, Darmochwał-Kolarz D. Plasma micro-RNA-22 is associated with disease activity in well-established rheumatoid arthritis. *Clin Exp Rheumatol*. 2022;40(5):945-51.
 32. Ormseth MJ, Solus JF, Sheng Q, Ye F, Song H, Wu Q, et al. The Endogenous Plasma Small RNAome of Rheumatoid Arthritis. *ACR Open Rheumatol*. 2020;2(2):97-105.
 33. Renman E, Brink M, Ärlestig L, Rantapää-Dahlqvist S, Lejon K. Dysregulated microRNA expression in rheumatoid arthritis families-a comparison between rheumatoid arthritis patients, their first-degree relatives, and healthy controls. *Clin Rheumatol*. 2021;40(6):2387-94.
 34. Cunningham CC, Wade S, Floudas A, Orr C, McGarry T, Wade S, et al. Serum miRNA Signature in Rheumatoid Arthritis and "At-Risk Individuals". *Front Immunol*. 2021;12:633201.
 35. Ormseth MJ, Solus JF, Sheng Q, Chen SC, Ye F, Wu Q, et al. Plasma miRNAs improve the prediction of coronary atherosclerosis in patients with rheumatoid arthritis. *Clin Rheumatol*. 2021;40(6):2211-9.
 36. Abdelaleem OO, Fouad NA, Shaker OG, Ahmed TI, Abdelghaffar NK, Eid HM, et al. Serum miR-224, miR-760, miR-483-5p, miR-378 and miR-375 as potential novel

- biomarkers in rheumatoid arthritis. *Int J Clin Pract.* 2021;75(11):e14651.
37. Lai NS, Yu HC, Tung CH, Huang KY, Huang HB, Lu MC. The role of aberrant expression of T cell miRNAs affected by TNF- α in the immunopathogenesis of rheumatoid arthritis. *Arthritis Res Ther.* 2017;19(1):261.
38. Li J, Ma L, Yu H, Yao Y, Xu Z, Lin W, et al. MicroRNAs as Potential Biomarkers for the Diagnosis of Chronic Kidney Disease: A Systematic Review and Meta-Analysis. *Front Med (Lausanne).* 2021;8:782561.
39. Wang B, Li Y, Hao X, Yang J, Han X, Li H, et al. Comparison of the Clinical Value of miRNAs and Conventional Biomarkers in AMI: A Systematic Review. *Front Genet.* 2021;12:668324.
40. Li SQ, Xie LY, Cai ZM, Wei HT, Xie MZ, Hu BL, et al. Systematic analyzing a five- miRNA panel and its diagnostic value of plasma expression in colorectal cancer. *Mol Biol Rep.* 2023;50(9):7253-61.
41. Garmaa G, Nagy R, Kóti T, To UND, Gergő D, Kleiner D, et al. Panel miRNAs are potential diagnostic markers for chronic kidney diseases: a systematic review and meta-analysis. *BMC Nephrol.* 2024;25(1):261.
42. Kim DH, Park H, Choi YJ, Im K, Lee CW, Kim D-S, et al. Identification of exosomal microRNA panel as diagnostic and prognostic biomarker for small cell lung cancer. *Biomarker Research.* 2023;11(1):80.
43. Wen Z, Li Y, Zhao Z, Li R, Li X, Lu C, et al. A serum panel of three microRNAs may serve as possible biomarkers for kidney renal clear cell carcinoma. *Cancer Cell International.* 2024;24(1):18.
44. Pigati L, Yaddanapudi SC, Iyengar R, Kim DJ, Hearn SA, Danforth D, et al. Selective release of microRNA species from normal and malignant mammary epithelial cells. *PLoS One.* 2010;5(10):e13515.
45. Yang QY, Yang KP, Li ZZ. MiR-22 restrains proliferation of rheumatoid arthritis by targeting IL6R and may be concerned with the suppression of NF- κ B pathway. *Kaohsiung J Med Sci.* 2020;36(1):20-6.
46. Zhang C, Fang L, Liu X, Nie T, Li R, Cui L, et al. miR-22 inhibits synovial fibroblasts proliferation and proinflammatory cytokine production in RASF via targeting SIRT1. *Gene.* 2020;724:144144.
47. Chang L, Zhou R. Histone methyltransferase EZH2 in proliferation, invasion, and migration of fibroblast-like synoviocytes in rheumatoid arthritis. *J Bone Miner Metab.* 2022;40(2):262-74.
48. Liu F, Wang Y, Huang D, Sun Y. LncRNA HOTAIR regulates the PI3K/AKT pathway via the miR-126-3p/PIK3R2 axis to participate in synovial angiogenesis in rheumatoid arthritis. *Immun Inflamm Dis.* 2023;11(10):e1064.
49. Liu W, Song J, Feng X, Yang H, Zhong W. LncRNA XIST is involved in rheumatoid arthritis fibroblast-like synoviocytes by sponging miR-126-3p via the NF- κ B pathway. *Autoimmunity.* 2021;54(6):326-35.